A study of the amorphisation reaction in Ni-Zr multilayers by neutron reflectometry

1990 J. Phys.: Condens. Matter 2 2537

(http://iopscience.iop.org/0953-8984/2/11/003)

J. Phys.: Condens. Matter 2 (1990) 2537–2545. Printed in the UK

A study of the amorphisation reaction in Ni–Zr multilayers by neutron reflectometry

A Zarbakhsh†, N Cowlam†, R J Highmore‡, J E Evetts‡, J Penfold§ and C Shackleton§

† Department of Physics, University of Sheffield, Sheffield S3 7RH, UK
‡ Department of Materials Science and Metallurgy, University of Cambridge, Pembroke Street, Cambridge CB2 3QZ, UK
§ Neutron Science Division, Rutherford Appleton Laboratory, Chilton, Didcot, Oxon OX11 0QX, UK

Received 18 April 1989, in final form 13 October 1989

Abstract. The critical neutron spectrometer, CRISP, at the ISIS pulsed neutron source at the Rutherford Appleton Laboratory has been used for an *in situ* study of the solid-state amorphisation reaction in sputtered multilayer Ni–Zr thin films heated to 235 °C in air. The variation of neutron reflectivity with wavelength observed for the samples shows very clearly a structure which changes during the reaction. This illustrates the considerable potential of the neutron reflectivity method.

1. Introduction

A new range of amorphous materials has been produced in recent years, by what have come to be known as 'solid-state process'—see Johnson *et al* (1985). These processes often involve the low-temperature heat treatment of an intimate mixture of two stable, elemental, crystalline components which leads to a metastable amorphous state. Although a number of phenomenological models have been proposed for such solid-state processes, the details of these reaction are not fully established. Diffusion at the interfaces between multilayer films is thought to be important and to depend on interface geometry and roughness. The first solid-state amorphisation reaction reported by Schwarz and Johnson (1983), was the formation of an amorphous AuLa alloy by the interdiffusion of polycrystalline gold and lanthanum thin films and the amorphisation of Ni–Zr multilayers has since been reported by the same group (Clemens *et al* 1984). The samples used in this work were Ni–Zr multilayers, which were prepared at Cambridge, in a getter sputtering system using a dual target DC magnetron system (Somekh *et al* 1984). An experiment was carried out using the critical reflection of neutrons, to determine the layer thicknesses and to observe the changes in the layer thicknesses due to interdiffusion, as the sample was heat treated on the neutron instrument.

2. Theory of neutron reflectivity

If a beam of long-wavelength neutrons is incident on a surface at small angles, the

0953-8984/90/112537+09$03.50

material appears as a continuous solid of refractive index n given by

$$n = 1 - \frac{\lambda^2 \bar{b}}{2\pi V}$$

where λ is the neutron wavelength, V the atomic volume and $\bar{b}$ the mean nuclear scattering amplitude. Total external reflection of neutrons can occur, when the glancing angle of incidence is less than certain critical value, because the refractive index for most media is less than unity. The critical glancing angle θ_c is given by

$$\theta_c = \lambda \left(\frac{\bar{b}}{V\pi} \right)^{1/2}.$$

If, however, the angle of incidence θ is greater than the critical angle θ_c, then the neutron beam will penetrate into the surface and for a specimen consisting of a sequence of layers this gives rise to interference effects which are analogous to the interference of light reflected from a series of parallel plates. Interference fringes then occur for values of neutron scattering vector Q which satisfy the equation

$$Q = 2\pi \frac{m}{d}$$

where m is an integer and d is the layer thickness.

Hence neutron reflectivity can be applied to the study of layer thicknesses and of scattering length density ($\bar{b}/V$) in thin film multilayer structures in the way discussed by Majkrzak (1986) who gives an example of an ideal reflectivity profile.

3. Experimental method and data analysis

The sample under investigation, consisted of 113 bilayers each consisting of 180 Å nickel and 180 Å zirconium deposited on to a rock-salt substrate using a dual target UHV DC magnetron sputtering system (Somekh *et al* 1984). The neutron experiment was carried out using the critical reflection spectrometer, CRISP, at the ISIS pulsed neutron source, employing a time-of-flight technique which enables the reflectivity profile to be measured in a fixed geometry. The resolution is determined only by the collimation and is essentially constant over the range of $\sin\theta / \lambda$ values used. The CRISP instrument (Penfold *et al* 1987, Felici *et al* 1987) consist of a single chopper with a 180° phaseable aperture which defines the wavelength band and partially removes the frame overlap contamination of successive pulses. The frame overlap for longer wavelength neutrons is removed by using an overlap mirror of nickel placed in the beam after the chopper. The beam collimation and size are determined by horizontal slits after the nickel mirror and before the sample. Neutrons from the sample are detected using a single ^{3}He gas detector after passing through a series of slits. A neutron beam monitor after the final slit, but just before the sample, is used to normalise the measured reflectivity data to the incident spectral shape.

A simple furnace was built for these preliminary measurements consisting of a large block with embedded heater elements and a thin semi-circular aluminium cover which was placed in position after initial alignment of the sample was performed using a laser beam along the neutron flight path. The furnace is shown schematically in

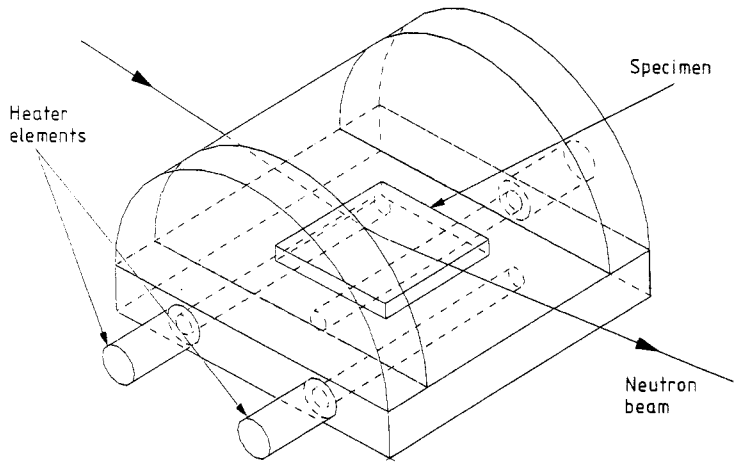

Figure 1. A schematic view of the annealing furnace used in the neutron experiments.

figure 1. The first experiment was carried out with the sample in the furnace at room temperature, with the angle of incidence at 0.4° and a wavelength range of 1 Å to 6.5 Å. Neutron counts were accumulated over 30 minutes and this experiment was done to determine the layer thicknesses, the scattering length densities and layer roughnesses of the as-received specimens.

The raw data were first corrected for the incidence spectral shape and detector efficiencies and the normalised data were set to an absolute reflectivity scale with reference of the region before the critical edge $\lambda > \lambda_c$ which is assumed to have unit reflectivity. The reflectivity profile obtained is shown in figure 2(*a*). It has a rather unusual form with a broad feature at $\lambda = 3.8$ Å almost reaching up to unit reflectivity. This feature is not the first-order Bragg peak from the multilayers which would actually be close to the critical edge, at $\lambda = 5$ Å. The second- and third-order Bragg peak are visible at $\lambda \sim 2.5$ Å and $\lambda \sim 1.7$ Å, respectively.

A series of simulations were made of these room-temperature data, using a computer program developed at the Rutherford Appleton Laboratory based on an optical matrix method (Penfold 1988). The simulation of the reflectivity profile for the expected thicknesses, 180 Å of nickel and 180 Å zirconium is shown in figure 2(*b*). The poor correspondence between experimental data and the simulation shows that the layer thicknesses differed from their expected values. A series of simulations was therefore carried out, varying the layer thicknesses, scattering length densities and surface roughness until a more reasonable fit was obtained. The parameters which appear to give the best fit were then used as a starting point for an iterative calculation using a least-squares fit until a refined set of parameters had been obtained. The bilayer model used gave a fit based on thicknesses of 161 Å of nickel and 252 Å of zirconium. This fit is not illustrated in figure 2 for reasons of space. Whilst being better than the line shown in figure 2(*b*), the fit was still very inaccurate in the region $4 < \lambda < 6$ Å. A second model consisting of nickel and zirconium layers with an amorphous Ni–Zr layer at their interfaces , was also used. This gave an improved fit, which is shown by the full curves in figure 2(*c*). It is based on 119 Å of nickel, 75 Å of a-Ni/Zr alloy and 137 Å of zirconium. The parameters obtained for the models are given in table 1.

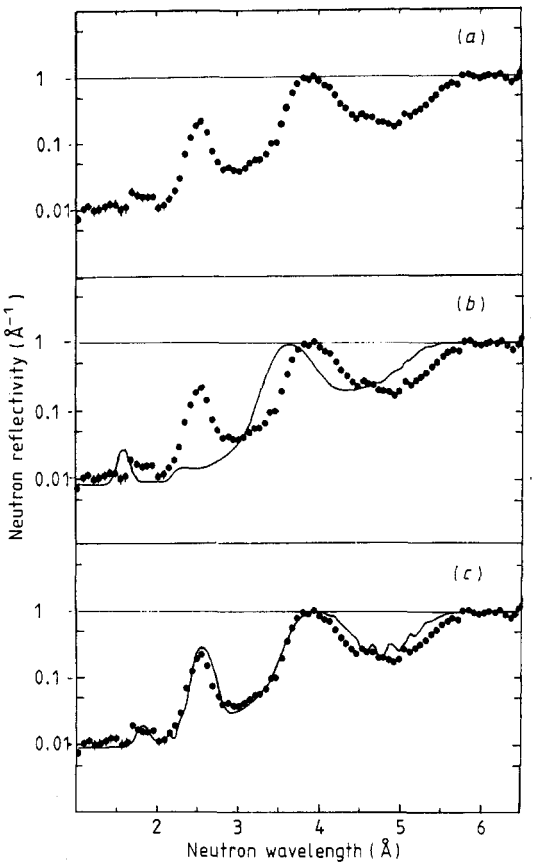

Figure 2. The normalised neutron reflectivity profile for the Ni–Zr multilayer sample at room temperature is given in (*a*) and shown below fitted with calculated curves: (*b*) a bilayer model with ideal layer thicknesses; (*c*) a model having nickel–zirconium alloy interfaces at each original layer. The parameters for these calculations are given in table 1.

A value for the instrumental resolution of around 8% was used in these fittings. The actual composition of these 180 Å / 180 Å samples was found to be 62% nickel and since equal thicknesses of nickel and zirconium occur at 68% nickel one expects the zirconium layers to be slightly thicker as observed.

Table 1. The parameters used in calculating the reflectivity curves shown in figure 2. The scattering length densities for nickel and zirconium are 9.40×10^{-6} Å^{-2} and 3.05×10^{-6} Å^{-2}, respectively.

Model	Layer	Thickness (Å)	b/V (10^{-6} Å^{-2})	Layer roughness (Å)
Ideal bilayer	Ni	180	9.40	0
(figure 2(*b*))	Zr	180	3.05	0
Bilayer with	Ni	116	9.30	38
a-NiZr interface	a-NiZr	76	4.20	38
(figure 2(*c*))	Zr	149	3.60	45

The results of these simulations show that even without any annealing, some interdiffusion at layer boundaries has taken place. This amorphisation could have been caused by the substrate being heated due to the energy from the target during the deposition, since the substrate has, for example, been found to attain to 115 °C during a three hour deposition run (Highmore *et al* 1988). An alternative but less likely explanation is that diffusion could have taken place at room temperature during the prolonged storage of the samples between their production and the neutron experiment. The values of layer roughness given in table 1 are derived from the least-squares fitting in the program. They are included in the model as a Gaussian of which the parameter is the standard deviation. Note that the values are lower than the 100 Å deduced for 'surface incursions' from the target spectrometry data on samples which were undergoing ion-beam etching (Clement *et al* 1984). We feel that the present measurements are more direct and the results in keeping with the expected quality of the interfaces.

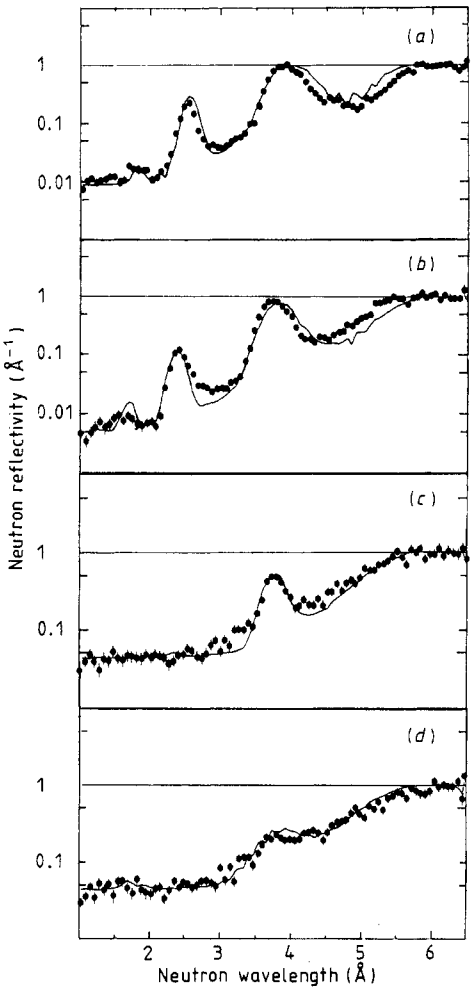

Figure 3. The normalised neutron reflectivity profiles for a Ni–Zr multilayer sample recorded in successive 30 min periods during annealing, fitted with calculated curves: (*a*) sample at room temperature; (*b*) the first period, mean temperature 143 °C; (*c*) the second period, mean temperature 225 °C; (*d*) the final period, mean temperature 235 °C.

After the room-temperature experiment, the alignment of the sample was repeated, the aluminium cover placed over it and the furnace heated slowly to 235 °C. The aim was to acquire data sets over sequential periods of 30 min. The relatively low annealing temperature was chosen in order that the amorphisation reaction should proceed to completion in a time of the order of 4 h (Newcomb and Tu 1986). In the event only half hour periods with mean temperature 143 °C, 225 °C and 235 °C were recorded before the observed signal degenerated. The reflectivity profiles obtained are shown in figure 3 and the evolution of these figure shows that layer thicknesses change and the distinctive layer structure disappears by the end of one and a half hour, as indicated by near extinction of the Bragg peaks. In detail it can be seen that the reflectivity profile at the end of the first period, 3(*b*), is similar to that for the room-temperature experiment 3(*a*). At the end of the second period, 3(*c*), the broad peak at $\lambda \sim 4$ Å has fallen in intensity and sharpened, while after the third period only a vestige of this peak remains in 3(*c*).

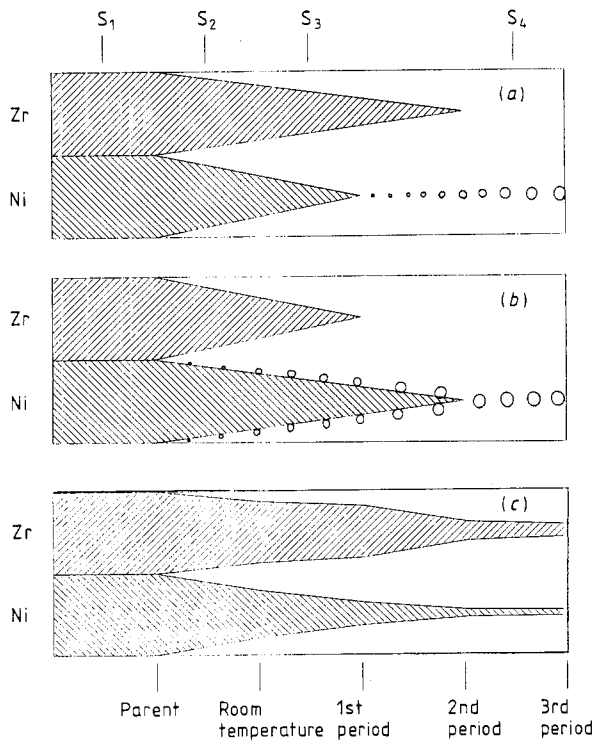

Figure 4. Schematic diagrams of the variation of Ni–Zr multilayer samples with time during solid-state reactions in which (*a*) the nickel and (*b*) the zirconium layers are consumed first. The circles represent voids. The four sections S_1 to S_4 are discussed in the text. (*c*) The scheme of the reaction as deduced from the neutron measurements.

In analysing these preliminary data, simple models were used, not least because there is a large number of instrument and sample variables in the fitting procedure and the interdependence of these variables is still being investigated. Two candidate models for the reaction are given in figure 4, which shows the change of thickness of the nickel, zirconium and a-NiZr layers with time. Figure 4(*a*) shows the scheme proposed by Schroder *et al* (1985) for ZrCo multilayers. In this, the layers of the rapidly diffusing species, here nickel disappear most quickly and finally leave just lines of voids. The nickel atoms are thought to diffuse quickly through the a-NiZr alloy to the zirconium / a-NiZr interface where the reaction proceeds. In figure 4(*b*) and alternative process takes place in which the zirconium layers are consumed first. This

model is suggested by the observation that a substantial population of voids occurs at the nickel / a-NiZr interface which must clearly influence the rate of mass transport at that interface. This observation has been interpreted as showing that 'a reduction in the overall thickness of the nickel layer occurs only in the initial stages of the reaction' (Newcomb and Tu 1986). The overall changes in multilayer structure in these two reactions can be considered in terms of the four labelled sections S_1 to S_4 in the figure which show, respectively, S_1, parent nickel and zirconium bilayers; S_2, nickel and zirconium with intermediate a-NiZr, four layers; S_3, nickel (or zirconium) alone with a-NiZr, bilayers; S_4, the end product a-NiZr only.

Table 2. The parameters used in calculating the reflectivity curves shown in figure 3 given in terms of bilayer Ni–Zr structures having amorphous NiZr alloy at the interfaces. These parameter are used as the basis for the schematic view of the reaction given in figure 4(*c*).

Layer	Thickness (Å)	b/V (10^{-6} Å^{-2})	Layer roughness (Å)
Room temperature			
Zr	149	3.60	45
a-Ni/Zr	76	4.20	38
Ni	116	9.30	31
Annealed at +143 °C for 30 min			
Zr	126	3.60	39
a-Ni/Zr	97	4.70	37
Ni	56	9.30	22
Annealed at +225 °C for 30 min			
Zr	46	3.60	37
a-Ni/Zr	162	5.80	30
Ni	18	9.30	21
Annealed at +235 °C for 30 min			
Zr	30	3.60	36
a-Ni/Zr	177	5.60	25
Ni	14	9.30	19

A series of fittings of the profiles in figure 3 were made sequentially using the layer sections S_1 to S_4, in order to determine the likely course of the reaction. The instrumental resolution was kept close to the value of 8% obtained for the room-temperature experiment and the scattering length densities started close to the values of nickel and zirconium. The fitted reflectivity profiles are shown by the full curves in figure 3 and the fitting parameters given in table 2. A scheme of the reaction is given in figure 4(*c*) which shows the steady growth with time of the a-NiZr intermediate layer, the more rapid disappearance of the nickel layers and that traces of both the nickel and zirconium layers remain in the specimen after the third period. A distinction between the two models of figure 4(*a*) and 4(*b*) can be made because the scattering length densities of the constituents are quite different, see table 1. The reflectivity profile of figure 3(*c*) is crucial since it is not possible to simulate this curve realistically if a substantial fraction of the nickel layers remain. In addition the final profile 3(*d*) is not consistent with either a fully transformed a-NiZr specimen nor just a single type of layer, nickel or zirconium, remaining. The scattering length densities obtained for

the layers given in table 2 are broadly as expected. The value for the zirconium layers is higher than for pure zirconium suggesting some admixture of nickel, while that for a-NiZr is roughly consistent with alloys of equiatomic concentrations, although the characteristic volume per atom, V, is not known. However, a more controlled experiment will be needed before reliable information on the composition of the a-NiZr layers can be obtained from such values. The incorporation of void layers into these simulations did not, incidentally, change the profiles significantly.

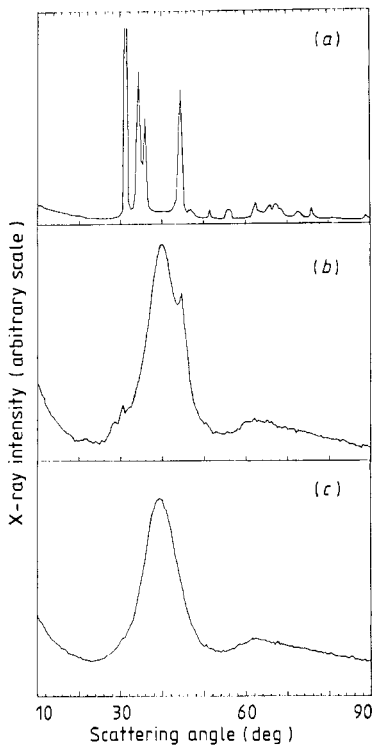

Figure 5. X-ray diffraction patterns for Ni–Zr multilayer specimens obtained with Cu Kα radiation: (*a*) unreacted 180 Å / 180 Å Ni–Zr multilayer; (*b*) the 180 Å / 180 Å sample used to obtain the graphs of figure 3 after the final period (small traces of treated nickel and zirconium remain); (*c*) a 90 Å / 90 Å Ni–Zr specimen of 272 periods fully transformed for comparison with (*b*).

The amorphisation reaction proceeded to completion more rapidly than expected and in the fitting of the final profile 3(*d*) it was necessary to increase the instrumental resolution to 18% for all the models tested. We were anxious therefore to establish that the changing shapes of the reflectivity profiles shown in figure 3 were genuinely attributable to the amorphisation process. The alternative possibility was that they were due to geometrical effects such as deterioration of the samples which were, of course, heated in air in these preliminary measurements. X-ray diffraction experiments using a Philips PW 1050 vertical diffractometer with a graphite curved crystal monochromator and copper Kα radiation were made on the samples at the end of the neutron experiments. The diffraction patterns showed that the samples were indeed amorphous and only small Bragg peaks corresponding to the zirconium {100} and nickel {111} reflections were observed, see figure 5. This indicates that small quantities of unreacted material were present in agreement with the reflectivity result shown in figure 4(*c*).

4. Conclusions

The conclusions of this preliminary investigation of the amorphisation reaction in Ni–Zr multilayers made by neutron reflectometry and annealing the samples in air can be summarised as follows:

(i) the data on the as-received samples were consistent with the reaction having already commenced, which we tentatively associate with sample heating during preparation.

(ii) the amorphisation reaction proceeded more rapidly than expected but this might have been a consequence of annealing the sample in air or the initially reacted state of the specimens.

(iii) a model in which the layers of the fast diffusing species nickel were consumed most rapidly provided that best overall fit to the data.

(iv) X-ray experiments showed that the Ni–Zr samples were almost wholly transformed after the annealing treatment. This indicates that the changes in reflectivity profiles were genuine effects and not caused by the deterioration of the samples.

A similar series of observations was, incidentally, made for a 90 Å / 90 Å multilayer sample having 272 periods and the neutron data for this sample are currently under analysis. X-ray diffraction showed that the amorphisation reaction was complete in this sample, which is expected to have shorter reaction time than the 180 Å / 180 Å specimen. We propose to make future experiments on these and other samples in order to quantify the changes produced by annealing, in ways that were not possible in this preliminary demonstration of the reaction process.

References

Clemens R M, Johnson W L and Schwarz R B 1984 *J. Non-Cryst. Solids.* **61–62** 817–822

Felici R, Penfold J, Ward R C and Williams W G 1987 *Rutherford Appleton Laboratory Report* RAL-87-047

Johnson W L, Atzmon M, Van Rossum M, Dolgin B P and Yeh X L 1985 *Proc. 5th Int. Conf Rapidly Quenched Metals* vol 2 (Amsterdam: North-Holland) pp 1515–1519

Highmore R J, Somekh R E, Greer A L and Evetts J E 1988 *Mater. Sci. Eng.* **97** 83–86

Majkrzak C F 1986 *Physica* B **136** 69–74

Newcomb S B and Tu K N 1986 *App. Phys. Lett.* **48** 1436–8

Penfold J 1988 *Rutherford Appleton Laboratory Report* RAL-88-088

Penfold J, Ward R C and Williams W G 1987 *Rutherford Appleton Laboratory Report* RAL-87-047

Schroder H, Samwer K and Koster U 1985 *Phys. Rev. Lett.* **54** 197–200

Schwarz R B and Johnson W L 1983 *Phys. Rev. Lett.* **51** 415–418

Somekh R E, Barber Z H, Baxter C S, Donovan P E, Evetts J E and Stobbs W M 1984 *J. Mater. Sci. Lett.* **3** 217–220